Experimental Study on the Mechanism of Turbulent Heat Transfer in Drag Reducing Flow by Surfactant Additives

F-Ch. Li*[1], Y. Kawaguchi* and K. Hishida**
* Turbomachinery Research Group, Institute for Energy Utilization, National Institute of Advanced Industrial Science and Technology, Tsukuba, 305-8564, Japan
** Department of System Design Engineering, Keio University, Yokohama, 223-8522, Japan
[1]Center for Smart Control of Turbulence

A drag-reducing surfactant solution flow in a two-dimensional channel is experimentally investigated. Simultaneous measurements of the velocity and temperature fluctuations in the thermal boundary layer are carried out. Two-component laser Doppler velocimetry (LDV) is used for measuring the velocity components and a fine-wire thermocouple probe for the temperature fluctuations at the same measurement location. The drag-reducing fluid tested is a dilute aqueous solution of a cationic surfactant, cetyltrimethylammonium chloride (CTAC), with 30 ppm concentration. Prior to measurement of the turbulent quantities, the gross flow characteristics of this drag-reducing solution are studied. The simultaneous measurements of velocity and temperature are made at inlet temperature of 31°C and at three different Reynolds numbers, Re = 3.5×10^4, 2.5×10^4 and 1.5×10^4, where the definition of Re is based on the channel height. The hydrodynamic and thermal turbulence structures and the turbulence productions and turbulence transport behaviors are then studied by analyzing the data sets of velocity and temperature fluctuations. The following terms are investigated: velocity and temperature statistics, Reynolds shear stress, turbulent heat fluxes in both the wall-normal and the streamwise directions, turbulence productions of both turbulent kinetic energy and temperature variance, eddy diffusivities for momentum and heat, and turbulent Prandtl number.

1. Introduction

The main objective of the present study is to clarify, through simultaneous measurements of instantaneous velocity and temperature fluctuations, the characteristics of turbulent structures of velocity and temperature fields in a drag-reducing flow by surfactant additives. The added surfactant gives functionality to the fluids and works to suppress turbulence. In this sense, the surfactant and micro-bubble have common feature to control the turbulence through the change of fluid property. This is the reason that the present work is expected to give hint to the analysis of turbulent bubbly flow.

Since the discovery of the dramatic drag-reducing effect of adding a small amount of certain high molecular weight water-soluble polymers or surfactants to water, the turbulence structures and mechanism of drag reduction (DR) in drag-reducing flow by additives have been intensively investigated in pipe, channel and boundary-layer flows. Some points of consensus have been obtained, such as the damping of fluctuations of the velocity component normal to the wall surface, enhancement of the streamwise velocity, attenuation of Reynolds shear stress due to the decorrelation between the wall-normal and streamwise velocity components, increase of the space between low-speed streaks near the wall and so on (Sadanandan and Sureshkumar 2002, Warholic et al. 1999, Hetsroni et al. 1997).

One of the most attractive applications of drag-reducing flow by additives is to reduce the pumping power required for circulating water in district heating and cooling (DHC) systems, especially by using surfactant additives. In such applications, polymer additives cannot be used because irreversible degradation of the drag-reducing ability of polymers generally occurs, caused by mechanical stress while passing through the circulating pump. However, when applying drag-reducing surfactants to a DHC system the heat transfer problem is inevitably encountered because the heat transfer rate of a drag-reducing flow by additives is also significantly reduced due to the dramatic suppression of turbulence (the heat transfer reduction, HTR, is usually so high as to be even larger than DR). Several attempts to enhance the heat transfer of drag-reducing flow by additives have appeared in the literature so far (Li et al. 2001, Fossa and Tagliafico 1995, Qi et al. 2001). Nevertheless, the problem of the contradiction between the heat transfer enhancement and the DR penalty of a drag-reducing flow by additives in industrial applications has not been solved adequately. Furthermore, the mechanism of the HTR itself in such drag-reducing flows has not yet been clarified. Therefore, the present experiments set out to clarify the turbulent thermal as well as hydrodynamic structures of a drag-reducing flow by surfactant additives, and thus clarify the heat transfer behaviors of such flow.

In the present study, experiments were carried out for the simultaneous measurement of the velocity and temperature fluctuations in the thermal boundary layer region in a drag-reducing surfactant solution flow in a two-dimensional (2D) channel. In Section 2, the experimental setup and measurement technique are described. The experimental results are presented in Section 3, for investigations on: the gross flow quantities under different temperatures and Reynolds numbers, and the influences of the drag-reducing surfactant additives on the respective characteristics of turbulence quantities, including the velocity and temperature statistics, the turbulent shear stress, $-\overline{uv}$, and the turbulent heat fluxes in both streamwise and wall-normal directions, $\overline{u\theta}$ and $-\overline{v\theta}$, the turbulence productions of both turbulent kinetic energy and temperature variance, $-\overline{u^+v^+}\left(\partial U^+/\partial y^+\right)$ and $-\overline{v^+\theta^+}\left(\partial \Theta^+/\partial y^+\right)$, eddy diffusivities for momentum and heat, $\upsilon_t = -\overline{uv}/\left(\partial U/\partial y\right)$ and $\alpha_t = -\overline{v\theta}/\left(\partial \Theta/\partial y\right)$, and turbulent Prandtl number, $\mathrm{Pr_t}$. The conclusions are given in Section 4.

2. Experimental setup and method

2.1 Facility

The closed-circuit water channel used in the present study is schematically depicted in Fig. 1. It is made of acrylic resin and has a straight part with length of 10 m, height (*H*) of 0.04 m and width of 0.5 m. An electromagnetic flow meter with uncertainty of ±0.01 m^3/min is installed in the upstream part of the channel for flow rate measurement. The wall shear stress is estimated from the static pressure difference between two fixed points on the wall in the streamwise direction, measured by a precise differential pressure gage with uncertainty of ±0.1 Pa. A tank with a volume of 2 m^3 serves as a reservoir for the working fluid and the temperature of the fluid in it can be controlled within ±0.1 K by a heating/cooling system. A honeycomb rectifier with length of 150 mm is set at the channel entrance for removing large eddies. The heating section has length of 0.9 m and is located at 8.2 m (measured from its front edge) downstream from the channel entrance, as shown in Fig. 2. Alternating current is used for the heating power. The measurement station is in the central plane in the spanwise direction and 0.8 m (20*H*) downstream from the front edge of the heating section, corresponding to 9.0 m (225*H*) downstream from the inlet of the channel. The coordinate system is given in Figs. 1 and 2.

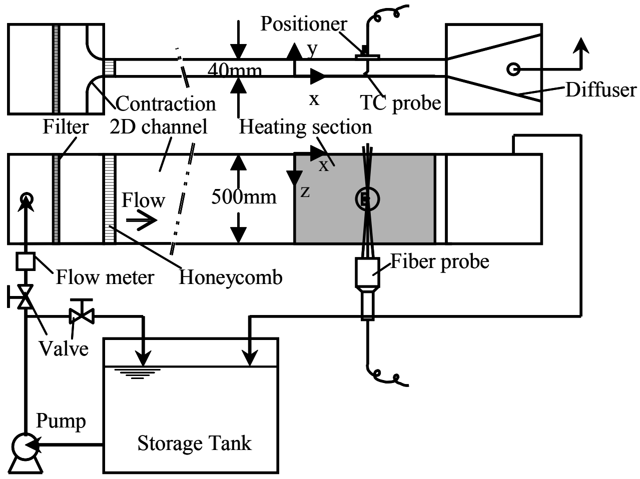

Fig. 1 Experimental facility and instrumentations

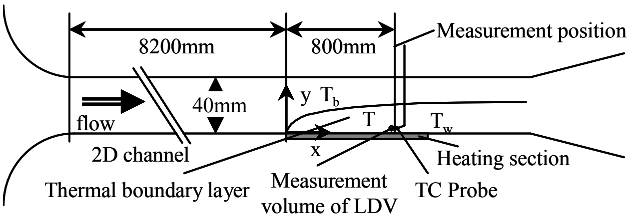

Fig. 2 Schematic diagram of the test section (top view)

2.2 Working fluids

A dilute aqueous solution (30 ppm) of a cationic surfactant, cetyltrimethylammonium chloride (CTAC) with chemical formula of $C_{16}H_{33}N(CH_3)_3Cl$, is prepared for the drag-reducing working fluid. The sodium salicylate (NaSal) is added to the solution with the same weight concentration as that of CTAC for providing counterions. Local tap water is used as the solvent. The thermo-physical properties of the solvent at the mean fluid temperature are used for data reduction for the dilute CTAC solution. Water is also used as the working fluid for comparison.

2.3 Measurement approaches

The velocity components in both the streamwise and the wall-normal directions are measured with a two-component LDV (two-color, three-beam mode) using 488 and 514.5 nm wavelengths of laser light. An argon ion laser (INNOVA 307C, Coherent Co.) is used as the light source. The dimensions of the measurement volume are 0.1, 0.1 and 3.6 mm in the streamwise, normal and spanwise directions respectively. The Doppler signals are processed with two synchronized burst spectrum analyzers (BSA 57N21, Dantec). The LDV measurement volume is positioned with a stage controller (Sigma Koki Co., Ltd.) in the wall-normal and spanwise directions within ±5 μm respectively and with a micrometric manipulator in the streamwise direction within ±1 μm.

The temperature fluctuations in the fluid are measured with a fine-wire thermocouple (TC) probe (K-type, Omega Co.). The fine-wire has a diameter of 25.4 μm (0.001 inch) and is supported by two prongs made of the same type of TC wire of diameter of 200 μm; the ratio of the diameter of junction to the wire is 3; and the time constant is estimated to be around 8×10^{-4} s (which is smaller than the Kolmogorov time scale, about 2.7×10^{-3} s) under the tested flow conditions. The output voltage signal of the fine-wire TC probe is amplified by a DC amplifier and the signals with frequency of higher than 1 kHz are screened out with a low-pass filter, before being sent to an analog digital converter (AD converter). The AD converter is synchronized with and triggered by the master BSA. The position of the fine-wire TC probe is controlled with a digital micrometric manipulator in the wall-normal direction within ±1 μm. The separation distance between the fine-wire TC junction and the LDV measurement volume is set to be 0.2 mm for all the runs (around 4η, where η is the Kolmogorov length scale estimated under the flow conditions), which has been proved to be an adequate choice. Note that Saarenrinne et al. (2001) showed that, away from the walls, grids of the order of 5η are sufficient for most purposes in numerical simulations, such as prediction of the mean flow and second moments of turbulence and all terms in the turbulent kinetic energy equation.

The heated-wall temperature of the heating section is measured with K-type TCs. All the TCs including the fine-wire TC probe are calibrated prior to the experiments and found to have uncertainty of ±0.1 K.

3. Results and discussion

It has been observed that the DR and HTR of a drag-reducing flow by additives strongly depend upon the fluid bulk temperature and flow rate (or Reynolds number) as well as the concentration of additives. The DR and HTR characteristics of the tested 30 ppm CTAC solution at different inlet temperatures and different flow rates are therefore investigated first. The velocity and temperature fluctuations are then simultaneously measured performed for several selected cases of the CTAC solution flows and water flows (see Table I for the test conditions). The turbulent characteristics and the turbulence transports in a drag-reducing flow by surfactant additives as well as in a water flow are investigated with the simultaneously measured velocity and temperature fluctuations. Around 1000 to 10000 synchronized data sets of the velocity and temperature, depending on the distance from the measurement location to the heated wall surface or on the data quality, are sampled for each case.

Table I. Test parameters

Case	T_{in}(℃)	Re($\times10^4$)	u_τ(m/s)	T_τ(℃)	DR (%)	HTR (%)
Water	31	2.5	0.025	0.020	-	-
CTAC (CA)	31	3.5	0.027	0.018	33.0	20.2
CTAC (CB)	31	2.5	0.012	0.041	70.0	77.3
CTAC (CC)	31	1.5	0.009	0.034	65.1	77.0

3.1 Gross flow characteristics

The relationships between the Fanning friction factor, f, Colburn factor, j_H, and Reynolds number, Re (based on the channel height, bulk velocity and viscosity of solvent), under different inlet temperatures are depicted in Figs. 3 and 4 respectively. Correspondingly, the DR and HTR values are plotted against Re in Fig. 5. The DR and HTR are defined as, $\mathrm{DR}=1-f/f_0$, and $\mathrm{HTR}=1-\mathrm{Nu}/\mathrm{Nu}_0$, where the Nusselt number, Nu, is based on the

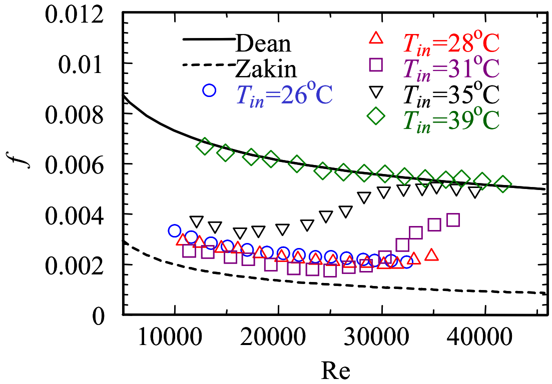

Fig. 3 Friction factor as a function of temperature and Reynolds number

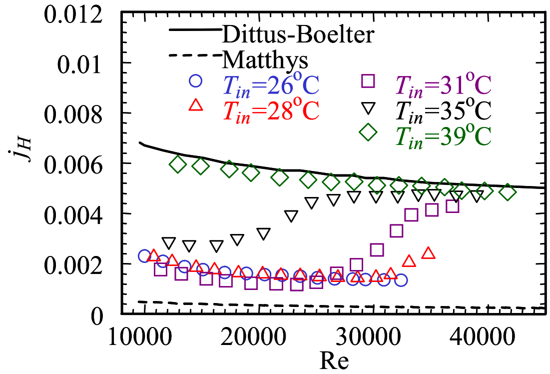

Fig. 4 Colburn j factor as a function of temperature and Reynolds number

channel height and the subscript "0" represents the solvent flow only. Dean's correlation of the friction factor for a Newtonian fluid in a 2D channel (Dean 1978), $f = 0.073\mathrm{Re}^{-0.25}$, and Zakin's lower limiting friction factor asymptote for nonpolymeric additive systems (Zakin 1996), $f = 0.315\mathrm{Re}^{-0.55}$, are included in Fig. 3. For the hydrodynamically fully developed but thermally developing water flow in a smooth channel, Gnielinski provided the following heat transfer correlation (Gnielinski 1976), $\mathrm{Nu}_D = 0.012\left(\mathrm{Re}_D^{0.87} - 280\right)\mathrm{Pr}^{0.4}\left[1 + (D/L)^{2/3}\right]$, where D is the hydraulic diameter of the channel, L the length of the heating section and Nu_D and Re_D respectively the Nusselt number and Reynolds number based on D. The Colburn factor calculated by using Gnielinski's correlation for water flow and Matthys's lower limiting Colburn factor asymptote for polymer solutions (Matthys 1991), $j_H = 0.03\mathrm{Re}^{-0.45}$, are also plotted in Fig. 4 for comparison. The tested inlet fluid temperatures are all in the effective drag-reducing range of the CTAC solution. For the 30 ppm CTAC solution flow presently tested, it is shown that the effective ranges of both the DR and HTR are near to 39°C. For the case of T_{in}=39°C, both f and j_H are close to those of a Newtonian fluid flow throughout the range of Reynolds number tested.

Seen from Figs. 3 and 4, f and j_H for the dilute CTAC solution flow decrease with the increase of Re and then reach a local minimum value. After that, the drag or heat transfer rate begins to gradually recover with the increase of Re, even the flow completely loses its drag-reducing or heat transfer reducing ability under a high enough Re (see the case of T_{in} = 35°C). The increase of DR or HTR before reaching the maximum value is thought to correspond to the process of forming so-called shear-induced structures (SIS). At a certain Re, at which the DR reaches its maximum value, the SIS may be in the most effective state for reducing drag. Above that, the threadlike network begins to break up under the high shear stress and the drag-reducing ability decreases (Lu et al. 1998).

For the present measured cases, the variation of DR and HTR after a local maximum value is the most striking under 31°C. The maximum DR for this case occurs at Reynolds number of around 2.5×10^4 (70%) and that of HTR at Reynolds number of 2.3×10^4 (79%), as plotted in Fig. 5.

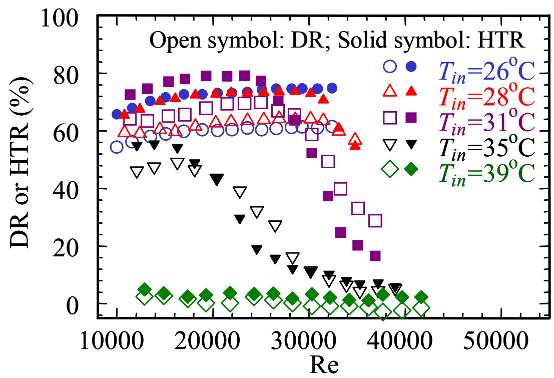

Fig. 5 DR and HTR as a function of temperature and Reynolds number

3.2 Effects of drag-reducing surfactant additives on turbulence statistics

3.2.1 Velocity statistics

The measured time-mean streamwise velocity (normalized by the friction velocity, $u_\tau = \sqrt{\tau_w / \rho}$, where τ_w is the measured wall shear stress) profiles for both the CTAC solution and water flows are presented in Fig. 6. Note that the superscript "+" represents normalization with inner variable(s) hereafter. It is clearly seen that the measured mean velocity profile for water flow is in close agreement with the turbulent velocity law-of-the-wall profile in the logarithmic region for Newtonian flow. For the CTAC solution flows, the velocity profiles in the near-wall region extend along with the laminar profile $U^+ = y^+$ to a more distant position compared with those of the Newtonian flow, which is one of the typical characteristics of drag-reducing flow by additives and is often referred to as the thickening of the inner region. The difference between the velocity profile of the drag-reducing CTAC solution flow and that of water in the logarithmic region increases with the DR level. The velocity profiles of the drag-reducing flow in the present experiment are all enclosed by Virk's ultimate curve (Virk 1975).

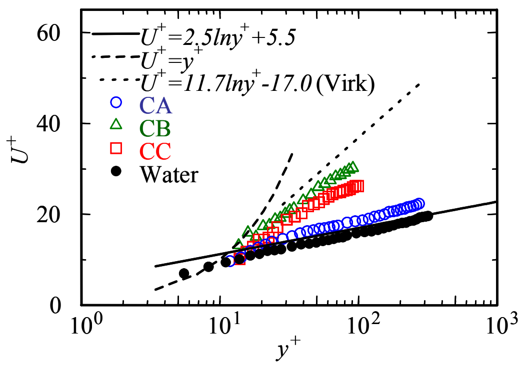

Fig. 6 Mean streamwise velocity profiles

The turbulent intensity profiles for the streamwise and wall-normal velocity fluctuations are shown in Figs. 7 and 8 respectively. It is seen that the location of the maximum value of u'^+ shifts to further away from the wall surface in the drag-reducing CTAC solution flow (from y^+ = 12 to y^+ =23-30) and the peak levels of u'^+ profiles are larger in drag-reducing flows compared to that in water flow. This is also a typical feature of the

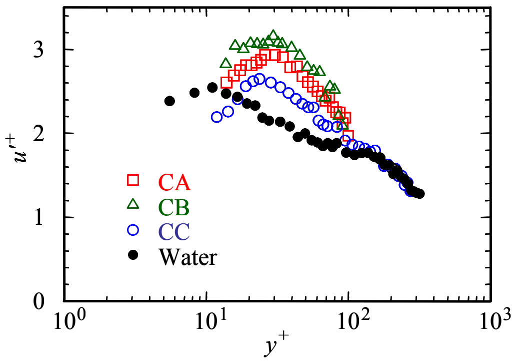

Fig. 7 Turbulent intensity profiles of streamwise velocity

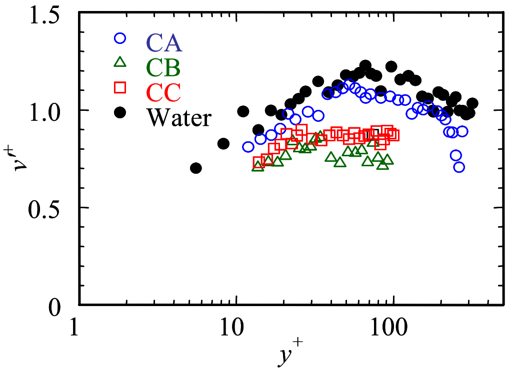

Fig. 8 Turbulence intensity of wall-normal velocity

drag-reducing flow by additives when the drag reduction is large enough. In contrast to the u'^+ results, the profiles of v'^+ for the drag-reducing surfactant solution flow, as shown in Fig. 8, are all depressed and the depression becomes more serious with the increase of DR level, which indicates the damping of the fluid motion normal to the wall by the drag-reducing surfactant additives. These results are consistent with those of previous studies on drag-reducing flow by either polymer or surfactant additives.

3.2.2 Temperature statistics

The profiles of the measured mean temperature difference ($\Theta = T_w$-T, where T_w is temperature of heated wall and T is fluid temperature) normalized by the friction temperature, $T_\tau = q_w / (\rho c_p u_\tau)$, where c_p is the specific heat capacity, for both water and the CTAC solution flows are plotted in Fig. 9. It shows that the mean temperature profile for water flow in the present measurement agrees quite well with Kader's correlation for Newtonian flow (Kader 1981). For the CTAC solution flows, however, the mean temperature profiles are significantly different from that of water flow. For cases CB and CC, it is clearly seen that a large temperature gradient exists when y^+ is smaller than about 50. In the experiments of drag-reducing fluid pipe flows carried out by Gasljevic et al. (2001), similar phenomenon was observed and they named this high-temperature-gradient layer as the elastic layer, which is analogous to the elastic layer of the velocity profiles in Virk's 3-layers model. In the outer region, the gradient of the temperature profiles becomes very small for the CTAC solution flow when the HTR level is high enough. The HTR of case CA is much smaller than those of CB and CC, and its temperature profile also varies from that of water flow but the change is still insignificant.

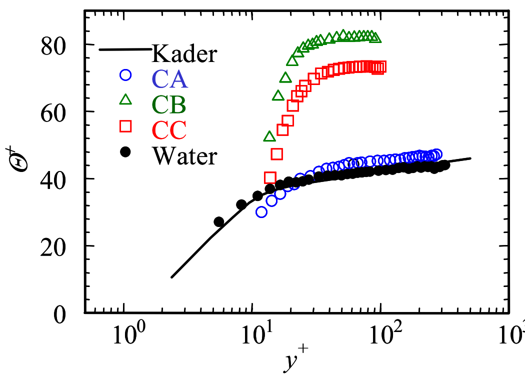

Fig. 9 Mean temperature profiles

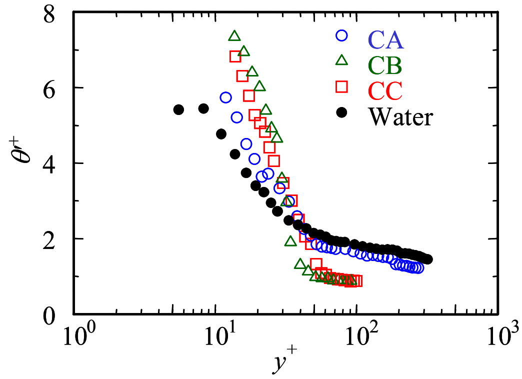

Fig. 10 Temperature fluctuation intensity

Figure 10 shows the profiles of the root-mean-square of the temperature fluctuations. Because the present experimental investigation focus on the coupling information of the velocity and temperature fluctuations, such as the turbulence transport for momentum and heat, the temperature measurement is also terminated when the LDV reaches its "acceptable measuring distance" very near to the wall. In the previous experiments (Li et al. 2002), the temperature profile was measured over a broader range in the close vicinity of the heated wall surface. The peaky structure of θ'^+ was clearly obtained. Similar to the velocity fluctuation profiles, the maximum values of θ'^+ also were larger for the drag-reducing CTAC solution flows and after those peaky points, θ'^+ dropped quickly until it became lower than that for water flow in the outer region. Although the turbulence intensity profiles of temperature fluctuations for CTAC solution flows do not show a peaky part within the range of the present measurements, Fig. 10 shows that the maximum value of θ'^{+} should be higher for the CTAC solution flows than that for water flow and the measured profile shows excellent repeatability compared to our previous experiment.

3.3 Effects of drag-reducing surfactant additives on turbulence transports

3.3.1 Turbulence transport for momentum

It has been confirmed by many investigators, both experimentally and numerically, that for drag-reducing flow by polymer or surfactant additives the turbulent momentum transfer could be significantly influenced by the additives, so the Reynolds shear stress profile would substantially decrease compared to that for a water flow. Furthermore, as stated by Hoyer and Gyr (1996), the reduction of the Reynolds shear stress is also the result of a decorrelation between the two velocity components involved in the calculation of the Reynolds shear stress term; the reduction of the turbulence intensity in the wall-normal direction alone would not completely explain the reduction in the Reynolds shear stress. Figure 11 shows the Reynolds shear stress profiles presently measured. The Reynolds shear stress for each of the three CTAC solution flows is less than that for the water flow, and the reduction of $-\overline{uv}$ evidently increases with the DR level. A decorrelation between u and v is also observed in our experiments, as shown in Fig. 12.

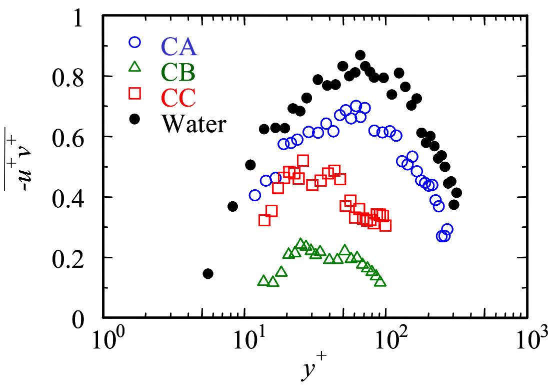

Fig. 11 Reynolds shear stress

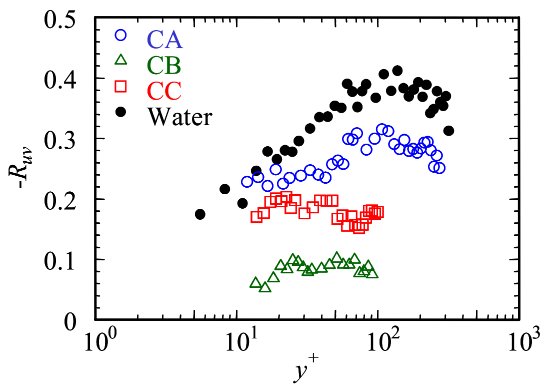

Fig. 12 Cross-correlation coefficients between u and v

In order to provide detailed information on the contributions to the total turbulence production from various events occurring in the turbulent flows, and to provide information on the influence of drag-reducing surfactant additives on such contributions, quadrant analysis (Lu and Willmarth 1973) of the Reynolds shear stress, $-\overline{uv}$,

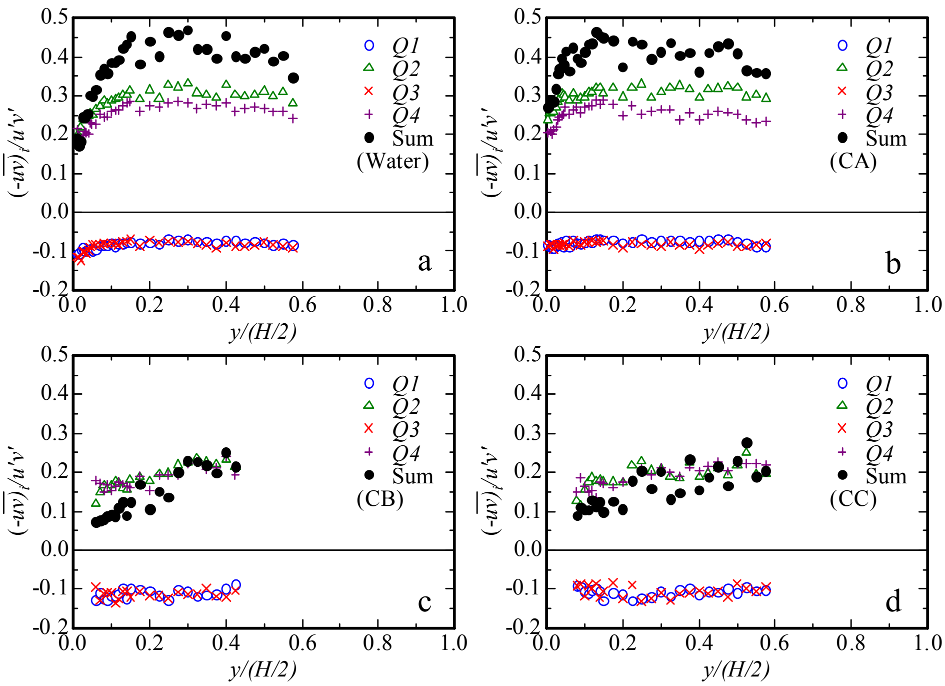

Fig. 13 Fractional contributions of the Reynolds shear stress from different quadrants.

has been conducted. The contribution of each quadrant to $-\overline{uv}$ is calculated with u and v only located in that individual quadrant in the velocity fluctuation coordinates (u, v) and is designated as $-\overline{uv_i}$ for the ith quadrant, where i = 1, 2, 3 and 4. Following Nagano and Tagawa (1988) and Kim et al. (1987), in the first quadrant $u > 0$ and $v > 0$, which represents outward interactions of fluid and is named $Q1$-motion; the second quadrant, $u < 0$ and $v > 0$, contains ejections of low-moment fluid from the wall ($Q2$-motion); the third quadrant, $u < 0$ and $v < 0$, contains wall-ward interactions of fluid ($Q3$-motion) and the fourth quadrant, $u > 0$ and $v < 0$, contains sweeps of high-moment fluid toward the wall ($Q4$-motion).

Figure 13 plots the distributions of $-\overline{uv_i}$ (i = 1, 2, 3 and 4), and the sum of these four terms that is equal to the Reynolds shear stress, for both water and drag-reducing CTAC solution flows. For the water flow, $Q2$ and $Q4$ motions are dominant in generating the turbulent shear stress, as clearly shown in Fig. 4a. Adding the drag-reducing additives to water, the turbulence transport behaviors are obviously changed. In all the three cases of CTAC solution flow, it is found that the distributions of $Q1$ and $Q3$-motions to the turbulent stress have nearly no differences from those in water flow, comparing Figs. 4b-4d with Fig. 4a. However, the contributions of $Q2$ and $Q4$-motions are changed significantly. With the increase of DR level, both $-\overline{uv_2}$ and $-\overline{uv_4}$ are depressed, so the sum, i.e., the turbulent shear stress, decreases in the drag-reducing flow. This indicates that the drag-reducing surfactant additives inhibit the processes of ejection of low-momentum fluid from the wall and the sweep of high-momentum fluid toward the wall, but do not affect the processes of both outward and wall-ward interactions of fluid.

3.3.2 Turbulence transport for heat

A. Turbulent heat flux in the wall-normal direction

Figure 14 shows the turbulent heat flux profiles in the wall-normal direction. It can be seen that the $-\overline{v^+\theta^+}$ profile has been depressed by the drag-reducing surfactant additives in the whole measured region and the depression increases with the HTR level. It is clear that the decrease of the Reynolds shear stress directly results in the drag reduction. It is conjectured that the heat transfer reduction may be due to the decrease of the wall-normal turbulent heat flux, for the wall-normal turbulent heat flux plays a similar role in the turbulence transport for heat as the Reynolds shear stress does in the turbulence transport for momentum. Additionally, from Fig. 14 and Fig. 11 the $-\overline{v^+\theta^+}$ profiles of the drag-reducing CTAC solution flows show a similar trend in variation as the $-\overline{u^+v^+}$ profiles. The term $-\overline{v^+\theta^+}$ seems to be influenced by the drag-reducing additives in the same way as the term $-\overline{u^+v^+}$, that is, the loss of correlation between the temperature and wall-normal velocity component fluctuations (one can see that the temperature fluctuation itself is locally enhanced by drag-reducing additives whereas $-\overline{v^+\theta^+}$ is depressed). The measured profiles of the cross-correlation coefficient between v and θ in both water and CTAC solution flows, as shown in Fig. 15, support the aforementioned conjectures obviously. Decorrelation between v and θ occurs. In addition, the profiles of $R_{v\theta}$ and R_{uv} exhibit similar shapes through the measured range, which also shows the similarity between the variations of $-\overline{uv}$ and $-\overline{v\theta}$ influenced by the drag-reducing additives.

Quadrant analysis is also conducted for $-\overline{v\theta}$ to understand the behavior of turbulence transport for heat in

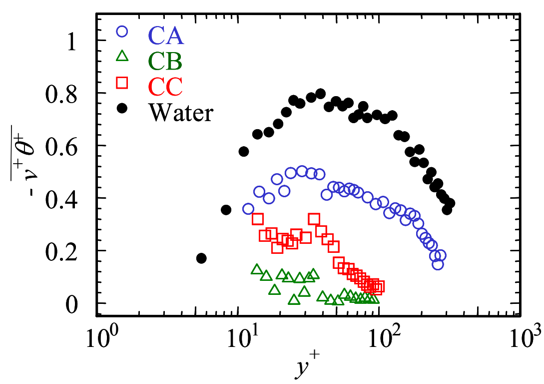

Fig. 14 Wall-normal turbulent heat flux

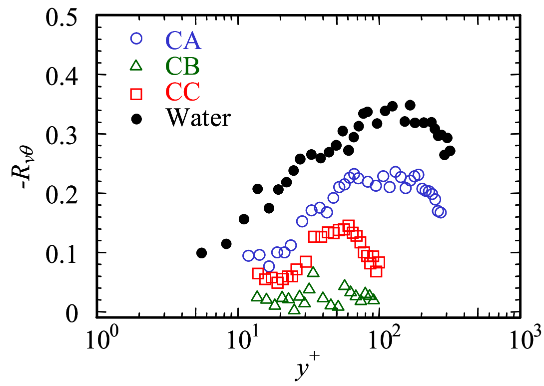

Fig. 15 Cross-correlation coefficient between v and θ

the drag-reducing flow. By calculating the fractional contributions to $-\overline{v\theta}$ from different quadrant-motions categorized in (u, v) plane, the influences of drag-reducing surfactant additives on thermal turbulence transport during different events, i.e., ejection, sweep and interactions, have been investigated.

Figure 16 shows the results of quadrant analyses of $-\overline{v\theta}$ for both water and CTAC solution flows. For

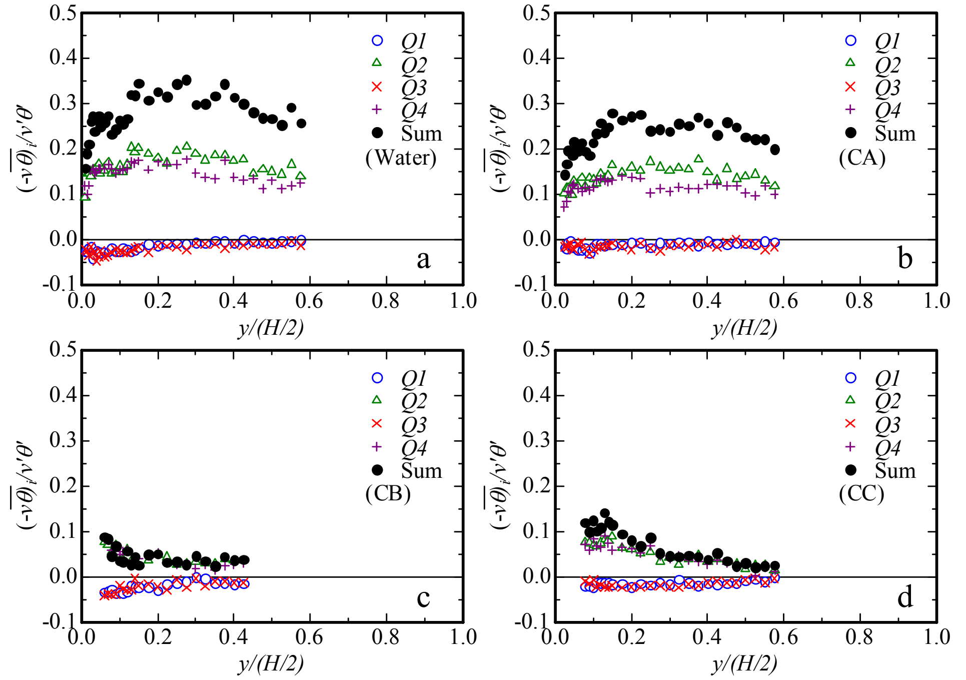

Fig. 16 Fractional contributions of wall-normal turbulent heat flux from different quadrants.

water flow, Fig.16a shows that contributions of $Q2$ and $Q4$- motions (ejection and sweep), to $-\overline{v\theta}$ are also predominant. The negative contributions of $Q1$ and $Q3$- motions (outward and wall-ward interactions) are quite low in absolute value (more evident if compared with those of $Q1$ and $Q3$ motions to $-\overline{uv}$). For the heated drag- reducing CTAC solution flow, it is observed that the fractional contributions of $Q2$ and $Q4$-motions are greatly decreased, but those of $Q1$ and $Q3$-motions do not have much change compared with those in water flow, which results in the depression of $-\overline{v\theta}$ in drag reducing surfactant solution flow. The decrease of contributions of $Q2$ and $Q4$-motions to $-\overline{v\theta}$ increases with the HTR level (Figs. 16B, 16C and 16D).

B. Turbulent heat flux in the streamwise direction

The measured profiles of turbulent heat flux in the streamwise direction, normalized by the friction velocity and temperature, are plotted in Fig. 17 for both water and CTAC solution flows. Comparing Fig. 17 with Figs. 7 and 10, it is seen that for the water flow the maximum value of $u^+\theta^+$ occurs at a location close to where the maximum values of u'^+ and θ'^+ occur (around 10 wall units). With the addition of drag-reducing additives to water, the profile of $u^+\theta^+$ is also enhanced in the region corresponding to the high-temperature-gradient layer. In addition, the enhancement of $u^+\theta^+$ is also due to the fact that u and θ do not lose their correlation in this layer in CTAC solution flow compared with that in water flow, which is confirmed by the cross-correlation coefficient between u and θ as shown in Fig. 18. Although the maximum values are not obtained in the limited measurement range for cases CB and CC (the peaky structure in the profile of $u^+\theta^+$ was observed in Li et al. 2002), it is evident from Fig. 17 that the maximum value of $u^+\theta^+$ in a drag-reducing flow by surfactant additives is enlarged and it increases with the HTR level. After the maximum value (cases CB and CC exhibit the tendency), the streamwise turbulent heat flux drops quickly to zero or even slightly negative value, where the

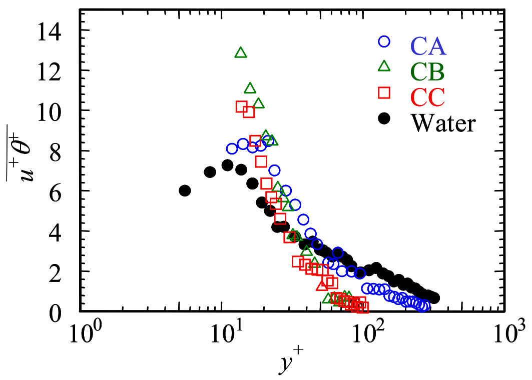

Fig. 17 Streamwise turbulent heat flux

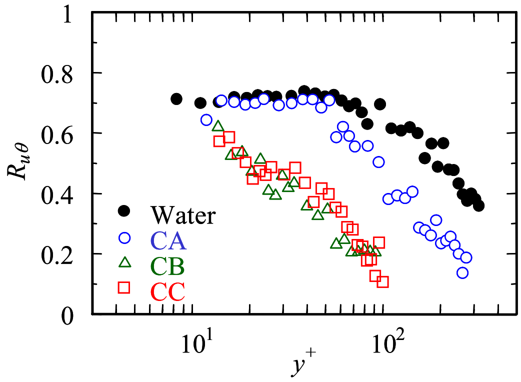

Fig. 18 Cross correlation coefficient between u and θ

cross-correlation of $R_{u\theta}$ is also significantly decreased (Fig. 18).

3.4 Effects of drag-reducing surfactant additives on turbulence productions

3.4.1 Production of turbulent kinetic energy

In the budget equation of turbulent kinetic energy, $\overline{u^+u^+}/2$, the production term is $-\overline{u^+v^+}\left(\partial U^+/\partial y^+\right)$, which is calculated from the measured Reynolds shear stress and the time-mean streamwise velocity profile. It can be deduced that $-\overline{u^+v^+}\left(\partial U^+/\partial y^+\right)\Big|_{\max} = 0.25$ for Newtonian fluid flow, at $-\overline{u^+v^+} = 0.5$ and $\partial U^+/\partial y^+ = 0.5$.

The influence of drag-reducing surfactant additives on the turbulence production of kinetic energy is shown in Fig. 19. Clearly, the production of kinetic energy is reduced in the drag-reducing CTAC solution flows and at high DR level (case of CB or CC) the reduction is quite significant. At the same time, the peaky structure moves away from the wall surface with increase of DR level. These results are in agreement with those obtained by other researchers in drag-reducing solution flows, e.g., Walker and Tiederman (1990) and Wei and Willmarth (1992) among others.

3.4.2 Production of temperature variance

The production term in the budget equation of temperature variance, $\overline{\theta^+\theta^+}/2$, reads as $\overline{u^+\theta^+}\left(\partial\langle T^+\rangle/\partial x^+\right) - \overline{v^+\theta^+}\left(\partial\Theta^+/\partial y^+\right)$. With the assumption of zero temperature gradient in the streamwise direction (e.g., as treated by Teitel and Antonia 1993), the turbulent energy production of temperature variance can be estimated once the wall-normal turbulent heat flux and the time-mean temperature profile are known. It can also be deduced that $-\overline{v^+\theta^+}\left(\partial\Theta^+/\partial y^+\right)\Big|_{\max} = \mathrm{Pr}/4$ for Newtonian fluid flow, at $-\overline{v^+\theta^+} = 0.5$ and $\partial\Theta^+/\partial y^+ = \mathrm{Pr}/2$.

Figure 20 shows the profiles of $-\overline{v^+\theta^+}\left(\partial\Theta^+/\partial y^+\right)$ in both water and drag-reducing CTAC solution flows. For water flow, the maximum value is 1.28, at $y^+ = 11$ in our measurement. Similar to the profile of production of turbulent kinetic energy, the production of temperature variance is also reduced by the drag-reducing additives. However, the reduction in the profile of $-\overline{v^+\theta^+}\left(\partial\Theta^+/\partial y^+\right)$ is not as significant as that in the profile of $-\overline{u^+v^+}\left(\partial U^+/\partial y^+\right)$ in the region corresponding to the high-temperature-gradient layer. Additionally, the peaky structure does not have a clear trend of moving away from the heated wall.

3.5 Effects of drag-reducing surfactant additives on turbulence diffusivity

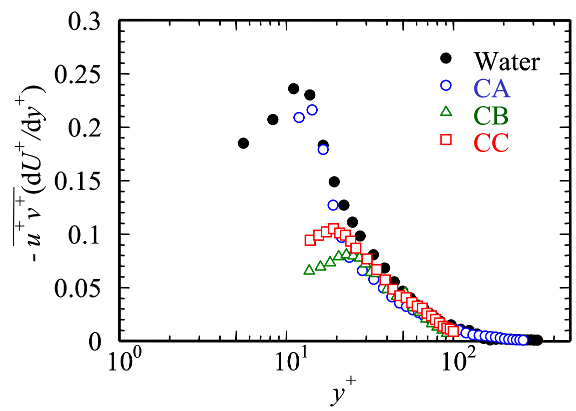

Fig. 19 Turbulence production of kinetic energy

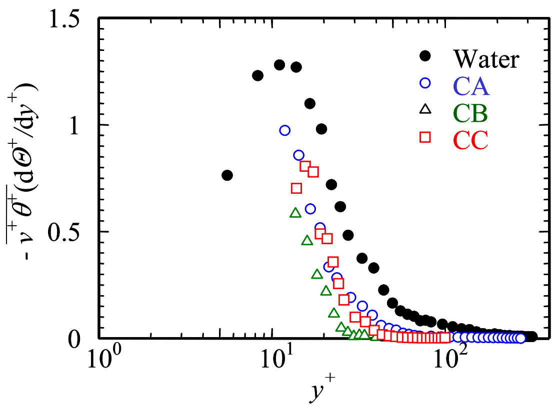

Fig. 20 Turbulence production of temperature variance

3.5.1 Eddy diffusivity for momentum and heat

The eddy diffusivities for momentum and heat are defined as $\upsilon_t = -\overline{uv}/\left(\partial U/\partial y\right)$ and $\alpha_t = -\overline{v\theta}/\left(\partial\Theta/\partial y\right)$.

Figure 21 shows the profiles of the momentum eddy diffusivity and Fig. 22 depicts those of the thermal eddy diffusivity. Note here that the figures show the dimensionless forms defined as $\nu_t^+ = -\overline{u^+v^+}/\left(\partial U^+/\partial y^+\right)$ and $\alpha_t^+ = -\overline{v^+\theta^+}/\left(\partial\Theta^+/\partial y^+\right)$.

It is found that the profiles of the eddy diffusivities for momentum and heat in the drag-reducing CTAC solution flows are both decreased across the whole measured range compared with those in the water flow. With the increase of the DR or HTR level, the depressions of ν_t^+ and α_t^+ profiles become more significant. These variation trends are consistent with those of the turbulence transport terms, such as the Reynolds shear stress and the wall-normal turbulent heat flux for the drag-reducing CTAC solution flows. On the other hand, it is seen that up to about y^+=50, the discrepancy from the water flow is more significant for the α_t^+ profile than that for the ν_t^+ profile, which results in the deviation of the turbulent Prandtl number profiles of the CTAC solution flows from that of the water flow, as explained below.

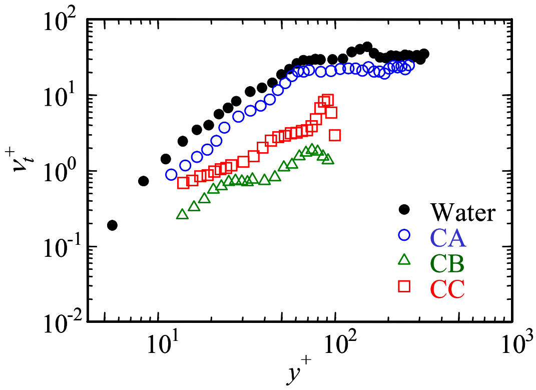

Fig. 21 Eddy diffusivity for momentum

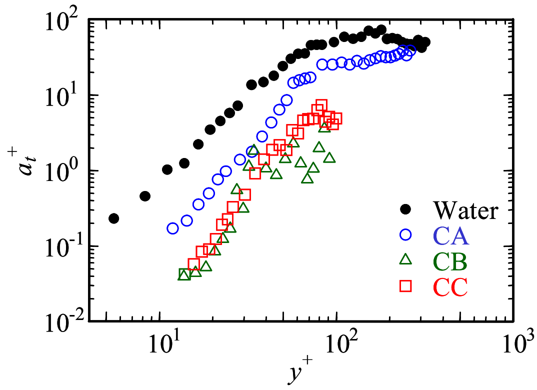

Fig. 22 Eddy diffusivity for heat

3.5.2 Turbulent Prandtl number

The turbulent Prandtl number is defined as the ratio between the eddy diffusivities for momentum and heat, $\mathrm{Pr}_t = \nu_t/\alpha_t = \overline{uv}/\overline{v\theta}\cdot(\partial\Theta/\partial y)/(\partial U/\partial y)$.

The calculated turbulent Prandtl numbers are shown in Fig. 23. For water flow, the $\mathrm{Pr_t}$ profile obtained in the present measurement shows a peak value of about 2.0, at 13.8 wall units. Away from this position, it drops to less than unity in the outer flow, which agrees in trend with the data measured by Kang et al. (2001) for the upward flow of liquid Refrigerant-113 in an annular channel, although the amplitude has some difference.

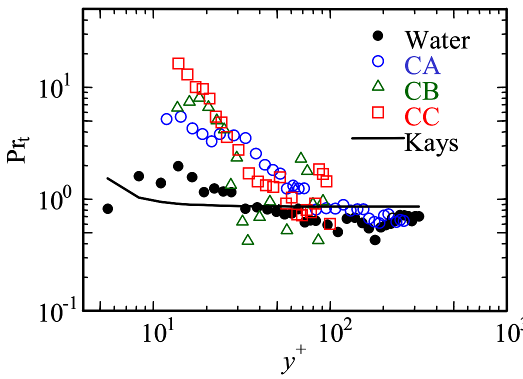

Fig. 23 Turbulent Prandtl number

For the drag-reducing CTAC solution flows, the estimated profiles of $\mathrm{Pr_t}$ are quite different from that of the water flow. From about y^+ = 50, the $\mathrm{Pr_t}$ profiles are close to that of the water flow. Approaching the wall surface from 50 wall units, $\mathrm{Pr_t}$ increases quickly till the measuring range (more than 10 wall units for the CTAC solution flows), which is just the consequence of the variation tendency of both the profiles of α_t^+ and ν_t^+. Recalling the mean temperature profiles shown in Fig. 9, it can be seen that the high turbulent Prandtl number region has good correspondence to the layer with high temperature gradient. Out of this high-temperature-gradient layer, the profiles of $\mathrm{Pr_t}$ in CTAC solution flow are in similar amplitude with that in water flow.

The feature of the profiles of $\mathrm{Pr_t}$ in CTAC solution flow in the near-wall region suggests that, near the heated wall, there must have been formed some unique fluid layers by the drag-reducing additives, which changed the flow state locally. Firstly, the high-temperature-gradient layer (Layer B) locating between y^+=10 and 50 is one of such unique layers, in which the eddy diffusivity for heat is much more depressed by the additives than that for momentum and $\mathrm{Pr_t}$ is enhanced. The eddy diffusivity for heat being smaller than that for momentum also means that the eddy transporting momentum does not efficiently transport heat in the aforementioned layer in CTAC solution flow. Temperature is therefore not a passive scalar anymore at least locally. Secondly, although we did not get information on the simultaneous velocity and temperature field in the close vicinity of the heated wall, it can be conjectured that there is another unique fluid layer (Layer A) in between the lower end of Layer B and the heated wall surface (i.e. y^+=0 to 10), which may change the flow state there and consequently affect the turbulence transport characteristics out of it. In the experimental study by Kawaguchi et al. (2001), the instantaneous temperature fluctuation in a heated CTAC solution flow was measured. The temperature profile was obtained in the very close vicinity of heated wall till about $y^+ = 1.5$. In layer A, heat diffusivity was evaluated to have large value because the mean temperature gradient in this layer showed very low. This high-thermal diffusivity layer in CTAC solution flow does not appear in Newtonian fluid flow. On the other hand, during the experiment, we visualized the very near-wall region in heated CTAC solution flow in the spanwise direction. Complicated simmering motions were found on the heated wall. The flow state could have been changed there, for example, when the network structures of the rod-like micelles in the solution were changed by heat, although recorded evidence is not provided herein. It needs energy to change the flow state. Therefore, the thermal energy supplied by the heated wall may be partly consumed by microstructures in the solution layer B. It is then conjectured that the interface of layer A and layer B corresponds to the interface of micellar phase change and consumes heat flux through the latent heat. These postulations remain to be evidenced by the future studies.

4. Conclusions

The following main conclusions are drawn from the present study:

A. The behaviors of friction factor and Colburn factor for the dilute surfactant solution flow tested show two kinds of critical phenomena, i.e., the existence of an upper critical temperature and an upper critical Reynolds number over which the flow loses the effectiveness of DR and HTR.

B. Typical hydrodynamic characteristics of drag-reducing flow by additives, such as expansion of the buffer layer, up-shift of the U^+ profile in the log-law layer, enhancement of u'^+ and depression of v'^+ were obtained. The thermal turbulence structure of such drag-reducing flow was also investigated. At high HTR level, a large temperature gradient appears when $y^+ < 50$ in the present measurement. The temperature fluctuation intensity, θ'^+, is also enhanced in the drag-reducing flow by surfactant additives.

C. The Reynolds shear stress is strongly decreased by drag-reducing additives. Quadrant analysis shows that the additives inhibit the processes of ejection of low-speed fluid from the wall and the sweep of high-speed fluid towards the wall, but do not affect the processes of both outward and wall-ward interactions of fluid.

D. Turbulent heat flux in the wall-normal direction is also strongly decreased in the heated CTAC solution flow. Quadrant analysis shows that the depression of $-\overline{v\theta}$ is resulted from the decreases of contributions of the second and fourth quadrant-motions, which is similar to the behavior happens to $-\overline{uv}$.

E. Turbulent heat flux in the streamwise direction in CTAC solution flow is enhanced in the region corresponding to the high-temperature-gradient layer, where u and θ do not lose much of their correlation.

F. The turbulence productions of turbulent kinetic energy and temperature variance are reduced in the drag-reducing CTAC solution flows. The former is reduced more significantly. The peaky structure in the profile of $-\overline{u^+v^+}\left(\partial U^+/\partial y^+\right)$ moves away from the wall, but that in the profile of $-\overline{v^+\theta^+}\left(\partial \Theta^+/\partial y^+\right)$ does not clearly show such a trend.

G. The profiles of the eddy diffusivities for momentum and heat in the drag-reducing CTAC solution flows are both decreased, which is consistent with the depression of the turbulence transport terms. The discrepancy from the water flow is more significant for the α_t^+ profile than that for the ν_t^+ profile in a region corresponding to the high-temperature-gradient layer. This directly results in the deviation of the turbulent Prandtl number profiles of the CTAC solution flows from that of the water flow in this layer.

References

Dean, R.B. 1978 Reynolds number dependence of skin friction and other bulk flow variables in two-dimensional rectangular duct flow. *J. Fluid Eng.* 100, 215.

Fossa, M. and Tagliafico, L.A. 1995 Experimental heat transfer of drag-reducing polymer solutions in enhanced surface heat exchangers. *Exp. Thermal Fluid Sci.* 10, 221.

Gasljevic, K. Aguilar, G. and Matthys, E.F. 2001 On two distinct types of drag-reducing fluids, diameter scaling and turbulent profiles. *J. Non-Newtonian Fluid Mech.* 96, 405.

Gnielinski, V. 1976 New equation for heat and mass transfer in turbulent pipe and channel flow. *Int. Chem. Eng.* 16, 359.

Hetsroni, G., Zakin, J.L. and Mosyak, A. 1997 Low-speed streaks in drag-reduced turbulent flow. *Phys. Fluids.* 9, 2397.

Hoyer, K. and Gyr, A. 1996 Turbulent velocity field in heterogeneously drag reduced pipe flow. *J. Non-Newtonian Fluid Mech.* 65, 221.

Kader, B.A. 1981 Temperature and concentration profiles in fully turbulent boundary layers. *Int. J. Heat Mass*

Transfer. 24, 1541.
Kang, S., Patil, B., Zarate, J.A. and Roy, R.P. 2001 Isothermal and heated turbulent upflow in a vertical annular channel-part I. Experimental measurements. *Int. J. Heat Mass Transfer.* 44, 1171.
Kawaguchi, Y., Daisaka, H., Yabe, A., Hishida, K. and Maeda, M. 2001 Structure of thermal boundary layer and heat transfer characteristics in drag reducing flow with surfactant additive. *Trans. Japan Soc. Mech. Eng.* 67(B), 1311.
Kim, J., Moin, P. and Moser, R. 1987 Turbulence statistics in fully developed channel flow at low Reynolds number. *J. Fluid Mech.* 177, 133.
Li, F-Ch., Kawaguchi, Y. and Hishida, K. 2002 Simultaneous measurements of velocity and temperature fluctuations in thermal boundary layer in a drag-reducing surfactant solution flow. *Exp. Fluids.* (Submitted).
Li, P., Kawaguchi, Y., Daisaka, H., Yabe, A., Hishida, K. and Maeda, M. 2001 Heat transfer enhancement to the drag-reducing flow of surfactant solution in two-dimensional channel with mesh-screen inserts at the inlet. *J. Heat Transfer.* 123, 779.
Lu, B., Li, X. Scriven, E. Davis, H.T., Talmon, Y. and Zakin, J.L. 1998 Effect of chemical structure on viscoelasticity and extensional viscosity of drag-reducing cationic surfactant solutions. *Langmuir* 14, 8.
Lu, S.S. and Willmarth, W.W. 1973 Measurements of the structure of the Reynolds stress in a turbulent boundary layer. *J. Fluid Mech.* 60, 481.
Matthys, E.F. 1991 Heat transfer, drag reduction, and fluid characterization for turbulent flow of polymer solutions; recent results and research needs. *J. Non-Newtonian Fluid Mech.* 38, 313.
Nagano, Y. and Tagawa, M. 1990 A structural turbulence model for triple products of velocity and scalar. *J. Fluid Mech.* 215, 639.
Nagano, Y. and Tagawa, M. 1988 Statistical characteristics of wall turbulence with a passive scalar. *J. Fluid Mech.* 196, 157.
Qi, Y., Kawaguchi, Y., Lin, Z., Ewing, M., Christensen, R.N. and Zakin, J.L. 2001 Enhanced heat transfer of drag reducing surfactant solutions with fluted tube-in-tube heat exchanger. *Int. J. Heat Mass Transfer.* 44, 1495.
Saarenrinne, P., Piirto, M. and Eloranta, H. 2001 Experiences of turbulence measurement with PIV. *Meas. Sci. Technol.* 12, 1904.
Sadanandan, B. and Sureshkumar, R. 2002 Viscoelastic effects on the stability of wall-bounded shear flows. *Phys. Fluids.* 14, 41.
Teitel, M. and Antonia, R.A. 1993 Heat transfer in fully developed turbulent channel flow: comparison between experiment and direct numerical simulations. *Int. J. Heat Mass Transfer*. 36, 1701.
Virk, P.S. 1975 Drag reduction fundamentals. *AIChE J.* 21, 625.
Walker, D.T. and Tiederman, W.G. 1990 Turbulent structure in a channel flow with polymer injection at the wall. *J. Fluid Mech.* 218, 377.
Warholic, W.D., Schmidt, G.M. and Hanratty, T.J. 1999 The influence of a drag-reducing surfactant on a turbulent velocity field. *J. Fluid Mech.* 388, 1.
Wei, T. and Willmarth, W.W. 1992 Modifying turbulent structure with drag-reducing polymer additives in turbulent channel flows. *J. Fluid Mech.* 245, 619.
Zakin, J.L., Myska, J. and Chara, Z. 1996 New limiting drag reduction and velocity profile asymptotes for nonpolymeric additives systems. *AIChE J.* 42, 3544.